Detailed look at aspects of optical pumping in sodium

J. J. McClelland and M. H. Kelley
Radiation Physics Division, Center for Radiation Research, National Bureau of Standards, Gaithersburg, Maryland 20899
(Received 21 February 1985)

Calculations and measurements are presented of the increase in $\bar{F}=1$ ground-state population as a function of incident laser intensity in optically pumped sodium. The calculations involve numerical integration of a multilevel version of the optical Bloch equations. Agreement between experiment and theory is good when proper account is taken of the residual Doppler width in the atomic beam, which causes a larger increase in the $\bar{F}=1$ population. The $\bar{F}=1$ population increases by 3.5% at 35 mW/cm^2, the highest laser intensity investigated.

I. INTRODUCTION

In recent years the preparation of atoms and molecules in definite quantum states has stimulated interest. Particular emphasis has been on creating a target for scattering experiments which has its spin and/or orbital angular momentum oriented along a particular direction.[1] Such a target, when used in conjunction with oriented scattering projectiles (such as polarized electrons, nuclei, or atoms) can provide detailed information on basic interactions (e.g., spin-orbit coupling and exchange) otherwise inaccessible when averaging over spatial orientation is necessary.

One of the most prevalent methods for state preparation of atomic targets has been the use of optical pumping with tunable dye lasers. Sodium, with its strong absorption on the D lines around 590 nm, is ideal for this method and hence has seen widespread experimental investigation[2–10] and a good deal of theoretical treatment.[7–10] As a result of this work, the basic principle by which a beam of sodium atoms is oriented by interaction with polarized resonant radiation is understood. Due to the arrangement of the hyperfine levels (see Fig. 1) incident σ^+ light tuned to the $\bar{F}=2\rightarrow F=3$ transition (causing only $\Delta M_F=+1$ transitions) creates a net movement of population from lower M_F to higher M_F, resulting in an accumulation in the $\bar{F}=2, M_F=+2$ ground state and $F=3, M_F=+3$ excited state (note that we use an overbar to indicate ground-state F sublevels and no overbar to indicate excited-state sublevels). Once atoms are in either of these two states, selection rules make transitions to other states impossible for pure circular polarizations of the light. The atoms can either be allowed to decay, in which case, being in the $\bar{F}=2, M_F=2$ state, they will be completely oriented ($\bar{F}=2, M_F=2$ implies both nuclear and electron spin point in the $+z$ direction, the direction of light propagation), or maintained in an oriented excited state[4] by continuing laser excitation.

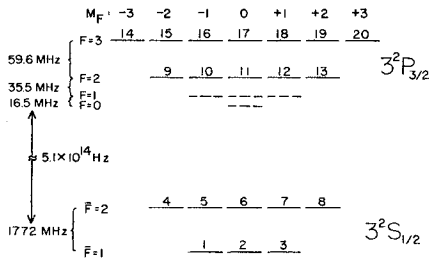

FIG. 1. Hyperfine structure of sodium, showing the numbering scheme used for the indices α, β, and γ in Eqs. (1)–(5).

Although this optical pumping principle has been shown to be basically correct, there are a number of experimental realities which make the exact degree of state selection of the sodium atoms difficult to predict. (1) Any weak magnetic field not oriented along the z axis causes a precession of the atomic angular momentum, corresponding to growth in population of other M_F sublevels. This problem is very important but can be reasonably well eliminated with suitable magnetic shielding or imposition of a guide field. (2) Variations of more than a few MHz in the pumping laser frequency can cause excess transitions to the $F=2$ excited state before optical pumping is complete. From this level, transitions are allowed to the $\bar{F}=1$ ground state, after which the atoms are lost to the pumping process. Depending on the laser bandwidth and stability, it is possible in a particularly bad case to pump almost all atoms to the $\bar{F}=1$ level before significant orientation is achieved. Use of commercially available frequency-stabilized, single-mode dye lasers, however, effectively circumvents this difficulty. (3) Any imperfection in the degree of circular polarization of the laser light causes continuous pumping in the negative M_F direction, resulting in a steady-state population which has not reached full orientation. Careful adjustment of optics and selection of windows with sufficiently small residual birefringence can keep this problem to a minimum as well.

Besides these experiental problems, there is a fundamental limitation which must also be considered. Even with perfect circular polarization, a stabilized laser with <1 MHz linewidth, and no magnetic field, a small fraction of the atoms is transferred to the $\bar{F}=1$ level during the transient period before the optical pumping is complete. This occurs because the $\bar{F}=2\rightarrow F=2$ transition has, in fact, a finite linewidth with a Lorentzian line shape and width (FWHM) of 10 MHz. The wing of this

line shape overlaps the $\bar{F}=2\rightarrow F=3$ transition with a small but not insignificant amplitude. As in (2) above, this opens the channel into the $\bar{F}=1$ level, where atoms are lost to the pumping process, causing an incomplete atomic polarization.

It is the purpose of this work to study in detail, both theoretically and experimentally, this last loss mechanism to the $\bar{F}=1$ level, in particular as a function of laser intensity. Since it is well known that any transition can experience power broadening, one would expect that, as the pump laser intensity is increased, the $\bar{F}=2\rightarrow F=2$ linewidth will increase, causing a greater transition probability in the wing overlapping the $\bar{F}=2\rightarrow F=3$ transition. This excessive laser intensity could cause additional loss to the $\bar{F}=1$ level, indicating that an optimum laser intensity should be found: it should be high enough to ensure complete optical pumping, but not so great as to reduce the orientation by increasing the loss to the $\bar{F}=1$ level.

II. THEORY

The proper framework in which to calculate the optical pumping of sodium has been the subject of some discussion. Formalisms exist which range from a very general multilevel atom interacting with an arbitrary intensity multimode laser field[11–14] to simple rate equation calculations.[1,8] As discussed by Hertel and Stoll,[1] the rate equation approach should be generally applicable to our situation if one wants to follow qualitatively the time evolution of the populations. However, we are interested in a phenomenon which depends critically on the details of the temporal behavior of transiently populated levels, the proper treatment of which requires detailed knowledge of the line shape as a function of time, as well as some accounting for coherence between the levels. Because a rate equation approach involves a somewhat *ad hoc* treatment of the line shape and allows for no coherence between states, we found it desirable to use a formalism which treats these effects implicitly from the outset. The simplest such method involves solving the optical Bloch equations for the elements of the density matrix. A complete discussion of this is provided by Yariv[15] and Allen and Eberly[16] for a two-level atom. We have taken their formalism and applied it in a limited way to the 20-level atom consisting of the $\bar{F}=1,\bar{F}=2$ ground state and $F=2,F=3$ excited-state sublevels. The $F=1$ and $F=0$ excited states were excluded to keep the number of equations down, on the grounds that their inclusion would not alter the results significantly since they are far off resonance and would have behavior similar to that of the $F=2$ level.

For the time evolution of the density matrix elements, we write

$$\dot{\rho}_{\alpha\beta}=-i\omega_{\alpha\beta}\rho_{\alpha\beta}-\frac{i}{\hbar}\sum_{\gamma}(H'_{\alpha\gamma}\rho_{\gamma\beta}-\rho_{\alpha\gamma}H'_{\gamma\beta}) , \tag{1}$$

where $\hbar\omega_{\alpha\beta}$ is the energy difference between the level α and the level β. The indices α, β, and γ run from 1 to 20 and correspond to the magnetic sublevels of the atom. The number scheme is shown in Fig. 1. $H'_{\alpha\beta}$ is the matrix element of the interaction Hamiltonian:

$$H'_{\alpha\beta}=\left\langle\alpha\left|\frac{e}{mc}\mathbf{A}\cdot\mathbf{p}\right|\beta\right\rangle , \tag{2}$$

which in the dipole approximation can be expressed as

$$H'_{\alpha\beta}=\sum_{\nu=\pm1,0}C^{\nu}_{\alpha\beta}\mu E\epsilon_{\nu}\cos(\omega_0 t) , \tag{3}$$

where μ is the dipole transition matrix element and $E\epsilon_{\nu}\cos(\omega_0 t)$ is the electric field for light with frequency ω_0 and polarization ν ($\nu=\pm1$ for $\pm$ circular polarization and $\nu=0$ for linear polarization). $C^{\nu}_{\alpha\beta}$ is the Clebsch-Gordan coefficient for the transition $\alpha\rightarrow\beta$, and is nonzero only when α and β denote states which are coupled by light of polarization ν.

To Eq. (1) we add the following phenomenological decay terms:

$$-\frac{1}{2\tau}\rho_{\alpha\beta}\ \text{ for }\dot{\rho}_{\alpha\beta}\ \ (\alpha\neq\beta) , \tag{4a}$$

$$-\frac{1}{\tau}\rho_{\alpha\alpha}\ \text{ for }\dot{\rho}_{\alpha\alpha}\ \ (\alpha\geq9) , \tag{4b}$$

$$+\frac{1}{\tau}\sum_{\beta=9}^{20}(C^{\nu}_{\alpha\beta})^2\rho_{\beta\beta}\ \text{ for }\dot{\rho}_{\alpha\alpha}\ \ (\alpha\leq8) . \tag{4c}$$

Equation (4a) is the decay term for the off-diagonals. They decay at half the rate of the diagonals, as discussed by Allen and Eberly.[16] Decay for the excited state levels is shown in Eq. (4b), while Eq. (4c) contains the increase in population of the ground-state levels due to spontaneous emission from the excited states. The quantity τ is the natural lifetime of the transition, taken to be 16 nsec.

The combination of Eqs. (1) and (4) yields 400 coupled differential equations in as many unknowns, whose solution gives the time evolution of all the populations of the atomic levels. Fortunately, several simplifications and approximations are possible which reduce the number of equations to 38 without too much loss of generality.

The most obvious simplification is to invoke the Hermiticity of the density matrix, which allows one to write $\rho_{\beta\alpha}=\rho^{*}_{\alpha\beta}$. This reduces the number of the equations by almost one half. The next step is to use the rotating-wave approximation (RWA),[16] in which all the off-diagonal elements are replaced by products of new variables $\sigma_{\alpha\beta}$ multiplied by $e^{i\omega_0 t}$, i.e., $\rho_{\alpha\beta}=\sigma_{\alpha\beta}e^{i\omega_0 t}$ $(\alpha\neq\beta)$. The result of this substitution is that some terms in the equations become slowly varying while others oscillate at optical frequencies. The basis for further approximation now lies in the assumption that any term which has optical frequency oscillation cannot be of physical significance and hence is assumed to average to zero. This allows many off-diagonal elements to be ignored. In fact, the only elements that remain are those which couple a ground-state level to an excited-state level. Off-diagonals coupling magnetic sublevels of a single F level are neglected, as are those connecting different F levels within the excited state or ground state. The effect of omitting these off-diagonals is to ignore some additional coherences which may develop, but which are assumed to play a secondary role in the present investigation.

As a slightly more limiting approximation, we have

also ignored the off-diagonals which connect the excited states to the $\bar{F}=1$ ground state. These extra elements were left out in the present case only because the calculation is aimed at relatively small laser powers and small detunings away from the $\bar{F}=2$ to $F=3$ transition. The terms can be expected to become important when the power broadening of the $\bar{F}=1\rightarrow F=2$ transition becomes large enough to have a significant amplitude at ω_0. By rough estimate this would be around 4 W/cm^2, which is a factor of 100—1000 larger than the powers considered in this study.

After these simplifications, the 18 off-diagonal matrix elements which are left combine with the 20 diagonal elements to form a complete set of 38 coupled differential equations. We write them down here in four categories.

(1) $\bar{F}=1$ ground-state diagonals:

$$\dot{\rho}_{\alpha\alpha}=\frac{1}{\tau}\sum_{\substack{\beta=9\\ \nu=\pm1,0}}^{20}(C^{\nu}_{\alpha\beta})^2\rho_{\beta\beta}\quad(\alpha=1-3)\,. \tag{5a}$$

(2) $\bar{F}=2$ ground-state diagonals:

$$\dot{\rho}_{\alpha\alpha}=-\frac{\mu E}{\hbar}\sum_{\substack{\beta=9\\ \nu=\pm1,0}}^{20}\epsilon_\nu C^{\nu}_{\alpha\beta}\mathrm{Im}\sigma_{\alpha\beta}+\frac{1}{\tau}\sum_{\substack{\beta=9\\ \nu=\pm1,0}}^{20}(C^{\nu}_{\alpha\beta})^2\rho_{\beta\beta}\quad(\alpha=4-8)\,. \tag{5b}$$

(3) Excited-state diagonals:

$$\dot{\rho}_{\alpha\alpha}=\frac{\mu E}{\hbar}\sum_{\substack{\beta=4\\ \nu=\pm1,0}}^{8}\epsilon_\nu C^{\nu}_{\alpha\beta}\mathrm{Im}\sigma_{\alpha\beta}-\frac{1}{\tau}\rho_{\alpha\alpha}\quad(\alpha=9-20)\,. \tag{5c}$$

(4) Off-diagonals:

$$\dot{\sigma}_{\alpha\beta}=i(\omega_{\alpha\beta}-\omega_0)\sigma_{\alpha\beta}-\frac{i\mu E}{2\hbar}\sum_{\nu=\pm1,0}\epsilon_\nu C^{\nu}_{\alpha\beta}(\rho_{\alpha\alpha}-\rho_{\beta\beta})-\frac{1}{2\tau}\sigma_{\alpha\beta}\,. \tag{5d}$$

The normalized amplitudes of light with ν polarization, ϵ_ν are obtained as follows:

$$\epsilon_{+1}=(I^{\sigma^+}/I_0)^{1/2}\,, \tag{6a}$$

$$\epsilon_0=0\,, \tag{6b}$$

$$\epsilon_{-1}=(I^{\sigma^-}/I_0)^{1/2}\,, \tag{6c}$$

where $I_0=I^{\sigma^+}+I^{\sigma^-}$. Since $\nu=0$ refers to light linearly polarized along the z axis, the direction of laser propagation, ϵ_0 must always vanish. The combination $\mu E/\hbar$ is equal to $0.554I^{1/2}$ (nsec^{-1}) for the sodium $3S_{1/2}\rightarrow 3P_{3/2}$ transition, where I is the laser intensity expressed in W/cm^2.

Equations (5) are solved numerically[17] with the initial condition that all ground-state diagonals have a value $\frac{1}{8}$ and all other elements are zero. The time dependent results are shown in Figs. 2 and 3 for $I=6$ mW/cm^2, the nominal two-level saturation intensity for the sodium $\bar{F}=2,M_F=2\rightarrow F=3,M_F=3$ transition. Qualitatively, the results are very similar to the rate equation results of Balykin,[8] with the exception of the $F=2$ excited state. The $\bar{F}=2,M_F=2$ ground state shows an initial dip, followed by an increase to a steady-state level of 0.46. The other sublevels decay at various rates as optical pumping

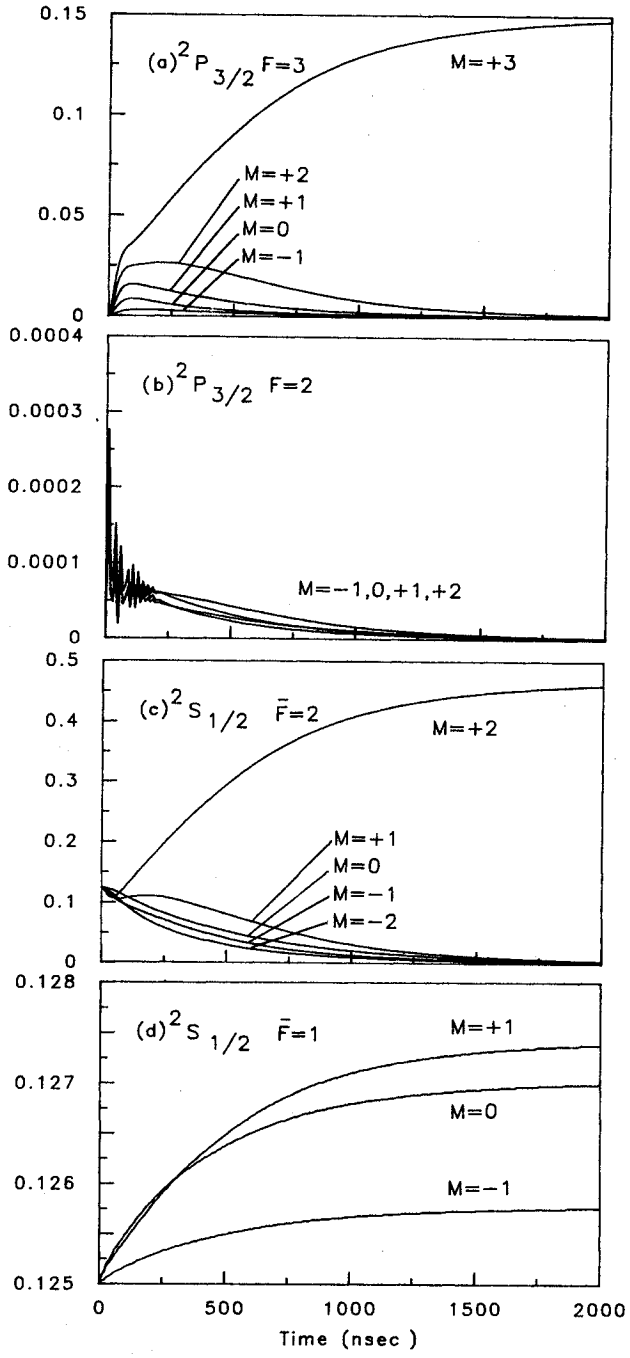

FIG. 2. Time dependence of the magnetic sublevel populations as calculated with the modified optical Bloch equations. The laser intensity is 6 mW/cm^2. (a) $^2P_{3/2}F=3$ excited state, (b) $^2P_{3/2}F=2$ excited state, (c) $^2S_{1/2}\bar{F}=2$ ground state, (d) $^2S_{1/2}\bar{F}=1$ ground state. Vertical axes represent fraction of atoms in each sublevel.

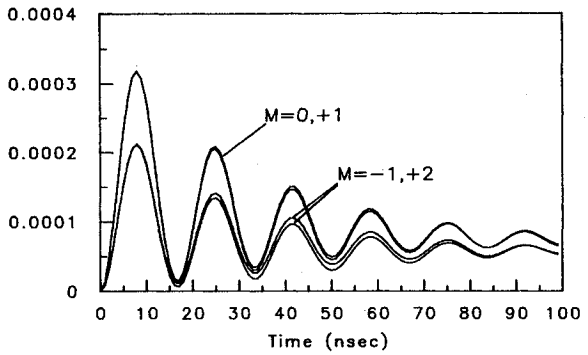

FIG. 3. First 100 nsec of Fig. 2(b), showing quasi-Rabi oscillations in the magnetic sublevel populations of the $^2P_{3/2}F=2$ excited state.

becomes complete. The $\bar{F}=1$ ground state sublevels all show a small increase, as expected, and the $F=3$ excited state sublevels all show a transient population except for the $M_F=+3$ level, which displays an increase to a steady-state value of 0.15. The $F=2$ excited state sublevels, on the other hand, have damped oscillatory behavior, which can be attributed to a form of Rabi oscillations. This phenomenon is a result of including coherence between ground and excited states and does not appear in rate-equation calculations.

III. EXPERIMENT

The experimental results shown here were obtained with two basic motivations. The first was to ascertain experimentally that there is no anomalously large loss to the $\bar{F}=1$ ground state during the optical pumping process. This is of interest for present experiments in which optical pumping is used for atomic state preparation. The second reason was to see how well the calculations described in the previous section do in predicting whatever loss does occur.

A schematic of the experimental setup is shown in Fig. 4. The sodium beam (density $\sim 10^{10}$ atoms/cm^3) and pump laser in an existing apparatus for spin-polarized electron-polarized atom scattering were used,[18] with the addition (downstream in the atom beam) of a second stabilized ring dye laser tuned to the sodium D_1 $(3S_{1/2}\rightarrow 3P_{1/2})$ $\bar{F}=1\rightarrow F=1$ transition to act as a probe. The fluorescence from this linearly polarized probe laser was taken to be proportional to the density in the $\bar{F}=1$ level, an assumption which is strictly correct regardless of any optical pumping by the probe laser, provided the isotopic distribution of the M sublevels in the $\bar{F}=1$ state is not significantly altered by the pump laser. The pump beam was locked to the $\bar{F}=2\rightarrow F=3$ transition by imaging its fluorescence spot onto a horizontally split photodiode. Due to the transverse Doppler shifts in the atom beam, any drift in laser frequency caused a movement of the spot and a corresponding change in the difference signal between the two halves of the diode. By connecting this difference signal to a feedback amplifier which controlled the frequency of the laser, the frequency could be kept within 1 MHz of the resonance line for periods of hours.

The pump and the probe lasers were chopped at frequencies of 75 Hz and 101 Hz, respectively, causing the resulting fluorescence signal from the probe region to consist of a 101-Hz square wave modulated by a small ampli-

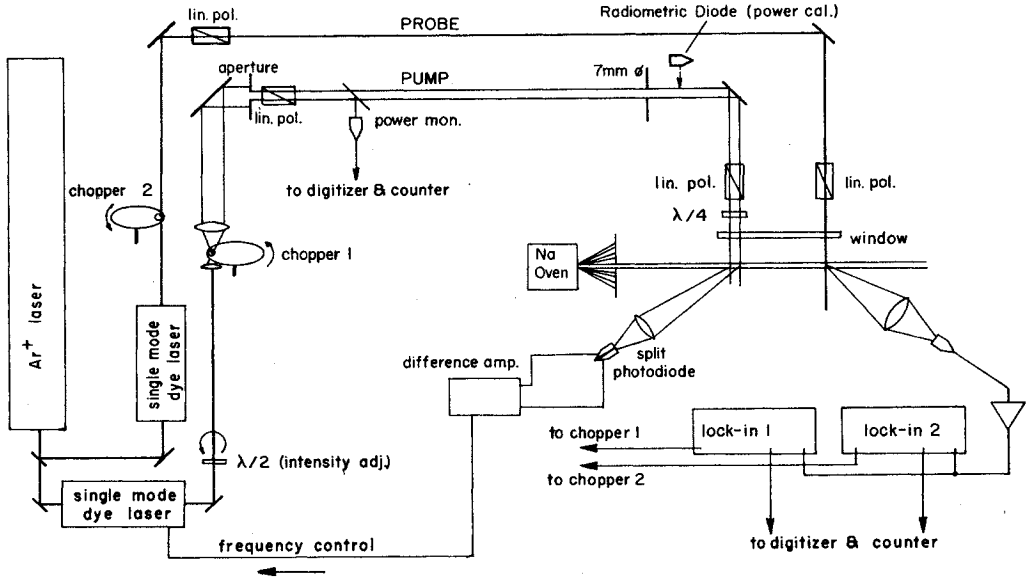

FIG. 4. Schematic of the experimental apparatus. Two single-mode dye lasers act as pump and probe as described in the text. The pump laser is tuned to the $^2S_{1/2}\bar{F}=2\rightarrow{}^2P_{3/2}F=3$ (D_2) transition, while the probe is tuned to the $^2S_{1/2}F=1\rightarrow{}^2P_{1/2}F=1$ (D_1) line. Pump and probe are chopped at different frequencies, allowing the probe intensity to be measured in one lock-in and the change in this intensity due to the pump laser in the other. The pump laser frequency is stabilized via a feedback loop coupled to a position sensitive diode, as discussed in the text.

tude 75-Hz square wave. This signal was connected simultaneously to the inputs of two lock-in amplifiers, referenced to the probe and the pump choppers. In this configuration, the signal S^{probe} from the amplifier locked to the probe-modulation frequency was proportional to the average amplitude of the probe fluorescence. The signal S^{pump} from the amplifier locked to the pump-modulation frequency was proportional to the change in this fluorescence due to optical pumping in the pumping region. These signals were corrected for background light by subtracting the signals from the two amplifiers remeasured with the probe laser sufficiently far off resonance that there was no fluorescence from the probe region. From the corrected signals the fractional increase in the $\bar{F}=1$ level was determined by

$$\delta=\frac{2S^{\text{pump}}}{2S^{\text{probe}}-S^{\text{pump}}}\ . \tag{7}$$

For each data point, the outputs of the lock-in amplifiers were digitized and counted for 20 1-sec intervals. The standard deviations of the means of these values were propagated through Eq. (7) and used as error bars (± 1 standard deviation) for the experimental measurements.

In order to avoid uncertainties in interpretation due to the pump-laser beam profile, the beam was expanded to 10 cm and only a 0.7-cm-diam central section was used, creating a constant radiation intensity across the pump region. The limiting aperture was approximately 30 cm from the atom beam. The power in the beam, varied by rotating polarizers with respect to each other, was monitored constantly by a photodiode which was calibrated before and after each experiment with a radiometric diode placed near where the beam entered the chamber. The calibration was then adjusted for a 10% loss in the mirror-circular polarizer unit and an 8% loss at the vacuum chamber window.

The circular polarizer, consisting of a Glan-Thompson linear polarizer and a zero-order $\frac{1}{4}$-wave plate was carefully adjusted and checked as follows. The circularly polarized light emerging from the unit was passed through a rotating linear polarizer. The resulting signal was measured with phase-sensitive detection at twice the frequency of rotation of the linear polarizer. The amplitude of the signal was compared to the signal obtained when the $\lambda/4$ plate was rotated 45° (creating linear polarized light). This measurement showed the degree of circular polarization to be $0.999\,80\pm0.000\,05$. Measurements on the window showed that the effect on this degree of circular polarization due to residual birefringence was not greater than ± 0.0003.

The results of four runs are shown together in Fig. 5. Not shown in the figure is an estimated systematic error in the calibration of the power of about $\pm 5\%$, due to slight variations in beam profile, diode sensitivity, etc. The behavior of the experimental curve is essentially as expected. At very low intensity, no optical pumping occurs and the population of the $\bar{F}=1$ ground state does not change. As the intensity is increased to about 5 mW/cm^2, we observe a rapid increase in the $\bar{F}=1$ population as optical pumping becomes important. The slope of the curve in this region is determined mainly by the distance over which the atoms interact with the pump laser. The longer this distance is, the more sharply the curve will rise, since the important quantity in determining the loss to $\bar{F}=1$ is the total number of photons absorbed. After 5 mW/cm^2, the pumping process is essentially complete and we observe only a gradual increase in the population as power broadening begins to become important. In this region, one expects that if power broadening did not exist, the curve would show no increase at all, since completed optical pumping means the loss mechanism to $\bar{F}=1$ is closed. The gradual increase which does occur is a reflection of the fact that the transition probability to $F=2$ during the transient period (before optical pumping is complete) is increasing with laser power as a result of power broadening.

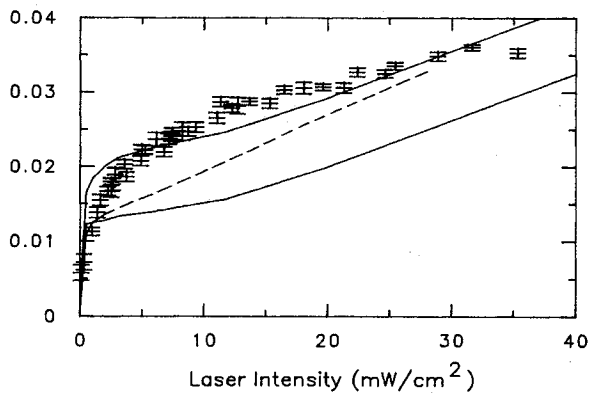

FIG. 5. Fractional increase in $\bar{F}=1$ population as a function of pump laser intensity. Lower solid curve: Calculation with no transverse Doppler width. Dashed curve: Calculation with 0.5% "wrong" polarization. Upper solid curve: Calculation with 10 MHz FWHM transverse Doppler width.

IV. COMPARISON OF THEORY TO EXPERIMENT

The calculated results shown in Fig. 2 represent the populations of the various levels of the sodium atom as a function of time, given that the laser power is turned on to a constant value at $t=0$. In order to cast these results in a form comparable to experiment, it was first necessary to average them over a finite transit time through the pump laser. Having taken some care in the experiment to make the laser beam constant in profile with sharp edges, it is a good approximation to say that all atoms fly at thermal speeds through the same region of uniform intensity. Thus their transit times are distributed according to the Maxwellian speed distribution associated with the temperature of the sodium oven exit nozzle. The resulting transit time distribution at 500°C rises sharply at 4 μsec, peaks around 9 μsec, and decays slowly, reaching 5% of its peak value at about 30 μsec. Using this distribution, and assuming that once the transit time has passed all excited states decay to the ground states according to their branching ratios, the fractional increase in $\bar{F}=1$ population was averaged to yield the lower solid curve in Fig. 5.

The more realistic upper solid curve in Fig. 5, which agrees well with the data, was obtained when the effect of

the small but finite residual Doppler width due to a small divergence of the atomic beam was included. Since, in a divergent atomic beam, different atoms have different velocity components along the laser beam, the atomic population is actually exposed to a distribution of frequencies, over which an average must be carried out. Fortunately, the numerical calculations show that over the range of incident intensities considered here, the fractional increase in $\bar{F}=1$ behaves very nearly parabolically as a function of laser detuning, for small detunings. The frequency dependence can then be parametrized and the average carried out analytically (assuming a Gaussian distribution of frequencies) at each intensity. The upper solid curve in Fig. 5 was created in this manner, using a 10-MHz FWHM frequency distribution. The value of 10 MHz was chosen as the best fit to the data, and it agrees reasonably well with an estimate of the true Doppler width (13 MHz).

In addition to taking into account the effect of the residual Doppler width, we also considered incomplete circular polarization of the pump laser in the calculations. A curve for 99% σ^+, 0.5% σ^- light is represented by the dashed line in Fig. 5. Interestingly, it seems that the two effects have very different influences on the fractional increase in $\bar{F}=1$. Improper polarization tends to make the slope of the curve larger, while the Doppler width essentially adds a constant to the curve. Since the data show no tendency toward a steeper slope, we did not consider incomplete light polarization further.

V. CONCLUSION

Two important conclusions can be drawn from this work. The first pertains to the practical application of optical pumping for atomic state selection. We have shown experimentally that at moderate laser intensity there can be complete atomic orientation of the $\bar{F}=2$ state with only a very small detrimental pile-up of population in the $\bar{F}=1$ ground state, provided reasonable care is exercised in eliminating magnetic fields, polarizing the laser, and stabilizing its frequency. Second, we have demonstrated that a numerical integration of multilevel optical Bloch equations can, even in a limited approach, produce results which agree reasonably well with experiments provided corrections for such effects as the residual Doppler width are taken into account.

That the results do not show absolute agreement within the error bars of the experiment is not surprising, considering the necessary simplifications and assumptions in the calculation. For example, no account has been taken of the atomic recoil induced by momentum transfer from the laser to the atoms, which can have two effects: (1) the atoms experience a Doppler shift as they recoil, and hence gradually go out of resonance with the laser by as much as 7–10 MHz; (2) faster atoms gain less transverse velocity than slower ones when traversing a constant distance of laser illumination. Thus the longitudinal velocity spread leads to more transverse velocity spread, increasing the Doppler width gradually along the pumping region to a value up to 20 MHz larger than the initial spread. Such effects further complicate the inclusion of the residual Doppler spread, already at best only semiquantitative because it rests on the assumption of a Gaussian line shape, which is certainly not exactly true. Nevertheless, despite these complications, it seems from considering the present results that a single Gaussian line shape is sufficient to describe all but the fine details of the behavior.

An obvious extension of this work is to investigate higher laser intensities and larger detunings. As mentioned above, it is a simple matter to include in the calculations the off-diagonal terms which couple the $\bar{F}=1$ ground state to the excited states. This should allow better treatment of higher laser intensities and would not create too large an increase in problem size. Clearly, however, to treat the problem for an arbitrary frequency and arbitrary powers, it will be necessary to retain all off-diagonal elements. At present this poses a difficulty in computational speed, but with further optimization of the code and use of high-speed computers the calculation is not inconceivable.

ACKNOWLEDGMENTS

The authors wish to thank R. J. Celotta for stimulating conversations. This work is supported in part by U.S. Department of Energy, Office of Basic Energy Sciences, Division of Chemical Science.

[1] I. V. Hertel and W. Stoll, Adv. At. Mol. Collisions **13**, 113 (1978).
[2] M. L. Citron, H. R. Gray, C. W. Gabel, and C. R. Stroud, Jr., Phys. Rev. A **16**, 1507 (1977).
[3] W. Dreves, W. Kamke, W. Broermann, and D. Fick, Z. Phys. A **303**, 203 (1981).
[4] A. Fischer and I. V. Hertel, Z. Phys. A **304**, 103 (1982).
[5] J. T. Cusma and L. W. Anderson, Phys. Rev. A **28**, 1195 (1983).
[6] W. Dreves, H. Jansch, E. Koch, and D. Fick, Phys. Rev. Lett. **50**, 1759 (1983).
[7] V. Kroop, Ch. Kammler, and W. Behmenberg, Z. Phys. A **286**, 139 (1978).
[8] V. I. Balykin, Opt. Commun. **33**, 31 (1981).
[9] P. G. Pappas, R. A. Forber, W. W. Quivers, Jr., R. R. Dasari, and M. S. Feld, Phys. Rev. Lett. **47**, 236 (1981).
[10] R. Walkup, A. L. Migdall, and D. E. Pritchard, Phys. Rev. A **25**, 3114 (1982).
[11] M. Ducloy, Phys. Rev. A **8**, 8144 (1973).
[12] J. Wong, J. C. Garrison, and T. H. Einwohner, Phys. Rev. A **13**, 674 (1976).
[13] A. M. F. Lau, Phys. Rev. A **14**, 279 (1976).
[14] T. H. Einwohner, J. Wong, and J. C. Garrison, Phys. Rev. A **14**, 1452 (1976).

[15]A. Yariv, *Quantum Electronics,* 2nd ed. (Wiley, New York, 1975).

[16]L. Allen and J. H. Eberly, *Optical Resonance and Two-Level Atoms* (Wiley, New York, 1975).

[17]R. F. Boisvert, S. E. Howe, and D. K. Kahaner, Routine CDRIV in *Guide to Available Mathematical Software,* Natl. Bur. Stand. publication NBSIR 84-2824 (Jan., 1984, NTIS Order PB84-171305).

[18]M. H. Kelley, W. T. Rogers, S. R. Mielczarek, and R. J. Celotta (unpublished).